

Efficient algorithms for autonomous electric vehicles' min-max routing problem

Seyed Sajjad Fazeli, Saravanan Venkatachalam, Jonathon M. Smereka

Abstract—Increase in greenhouse gases emission from the transportation sector has led companies and government to elevate and support the production of electric vehicles. The natural synergy between increased support for electric and emergence of autonomous vehicles possibly can relieve the limitations regarding access to charging infrastructure, time management, and range anxiety. In this work, a fleet of Autonomous Electric Vehicles (AEV) is considered for transportation and logistic capabilities with limited battery capacity and scarce charging station availability are considered while planning to avoid inefficient routing strategies. We introduce a min-max autonomous electric vehicle routing problem (AEVRP) where the maximum distance traveled by any AEV is minimized while considering charging stations for recharging. We propose a genetic algorithm based meta-heuristic that can efficiently solve a variety of instances. Extensive computational results, sensitivity analysis, and data-driven simulation implemented with the robot operating system (ROS) middleware are performed to corroborate the efficiency of the proposed approach, both quantitatively and qualitatively.

Index Terms—Autonomous Electric Vehicles, Routing, Charging Station, Genetic Algorithm, Variable Neighborhood Search, Robot Operating Systems

I. INTRODUCTION

Global warming has been primarily linked to human activities which release greenhouse gases [1]. Among those activities, the transportation sector causes the largest share (about 28%) of greenhouse gas emissions, which mainly originate from fossil fuel burner vehicles [2]. In an effort to offset carbon emissions from fossil fuel burning vehicles, priority to transform the transportation systems by driving new technological innovations in vehicles [3] is causing electronic vehicles (EVs) to become rapidly important for many automotive companies. Many countries have offered incentives to accelerate the adoption of EVs to increase the EV share in future vehicle fleets [4]. Meanwhile, autonomous driving technologies are evolving and considerable efforts are made to advance the real-world applications for self-driving [3].

Due to natural synergies between the autonomous and EVs, automotive companies are striving to equip the EVs with autonomous driving technologies [5]. Autonomous electric vehicles (AEV) have capabilities for decision making, on-board computation, and connectivity. It is important for AEVs to choose energy-efficient routes and find the best locations

for recharging during their itineraries. Transportation network companies (e.g., Lyft and Uber), and logistic companies (e.g., FedEx and UPS) seek to operate a fleet of AEVs in their business in the future [6]. Adopting AEVs also brings new challenges. One of the main operational challenges for AEVs in transport applications is their limited range and the availability of charging stations (CS) [7]–[9]. It is estimated that half of the US population lives in areas with fewer than 90 charging infrastructures per million people [10], [11]. To successfully employ AEVs, we need strategies that can alleviate the range and recharging limitations.

The autonomous electric vehicle routing problem (AEVRP) with limited range and number of CSs presented in this work, falls into the category of green vehicle routing problem (GVRP). The GVRP embraces a broad and extensive class of problems considering environmental issues as well as finding the best possible routes for vehicles. The GVRP research can be broadly divided into two categories: 1) minimize the fuel consumption while considering loading weights [12]; and 2) replace the conventional vehicles with Alternative Fuel Vehicles (AFV) [8], [13]–[16]. This research focuses on AFVs, hence we briefly review the related literature on routing strategies for AFVs. An initial work was done by [17], where the authors developed a mixed integer programming (MIP) formulation and a genetic algorithm meta-heuristic to overcome the range limitation of AFVs and shortage of refueling locations. Authors in [8] introduced the EV routing problem with time windows and charging stations with the limited freight capacity for the vehicles. They developed a hybrid meta-heuristic by integrating variable neighborhood and tabu search. For single unmanned aerial vehicles' routing problem, authors in [13] proposed a novel approach based on an approximation algorithm combined with a heuristic method. Later, the authors extended their work to multiple vehicles by applying the Voronoi algorithm as the construction phase, and 2-opt, 3-opt variable neighborhood searches in the improvement phase [18].

In this work, we define the AEVRP as follows: given a set of AEVs which are initially stationed at a depot, a set of targets and a set of CSs, the goal is to visit each target exactly once by any AEV and return to the depot while no AEV runs out of charge while they travel their respective routes. We assume that all AEVs will be fully charged at any visited CS, and the fuel consumption rate is linearly proportioned with traveled distance. This research considers a variant of the AEVRP, which we refer to as min-max AEVRP. The objective of this problem is to minimize the maximum distance traveled by any AEV instead of the total distance (min-sum), which is

S.S. Fazeli and S. Venkatachalam are members of the Department of Industrial and Systems Engineering at Wayne State University, Detroit, MI. J. M. Smereka is a researcher within the Ground Vehicle Robotics (GVR) team at the U.S. Army CCDC Ground Vehicle Systems Center (GVSC) in Warren, MI, (e-mail: sajjad.fazeli@wayne.edu; saravanan.v@wayne.edu; jonathon.m.smereka.civ@mail.mil), Corresponding author: S.Venkatachalam. Distribution A. Approved for public release; distribution is unlimited. OPSEC # 4492.

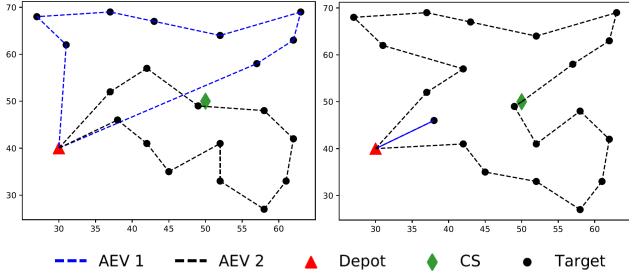


Fig. 1: A feasible tour for two AEVs visiting all the targets while visiting some charging stations for recharging: AEVRP using min-max (left) vs min-sum (right).

conventional in VRP. The min-max AEVRP is fundamentally different from min-sum AEVRP. An optimal solution in min-max AEVRP assigns routes to all AEVs such that none of the AEVs has a longer route. This will result in a more balanced distribution of loads and fair and equitable utilization of the AEVs, which can decrease the rates of battery degradation in AEVs [19]. Refer to Fig. 1 for an illustration for min-max and min-sum routes for AEVs. In Fig. 1, AEV1 visits most of the targets and travels a lot of distance compared to AEV2 with min-sum. However, using min-max, the two AEVs travel almost the same amount of distance.

The min-max AEVRP is also of interest when the time to visit every target from the base depot is more important than the total traveled distance in applications like surveillance, emergency and disaster management [20], intelligence, surveillance, and reconnaissance [21]–[23], and multi-robot path planning problems. In energy-efficient multi-robot path planning the goal is to obtain optimal paths for each robot while avoiding obstacles in the presence of recharging points [24]. Additionally, the min-max provides a fair and equitable utilization for the resources, and the maximum wait time of the targets will be less compared to a solution from min-sum. This is particularly vital if the AEVs are used to transport people, and the targets are considered as stops in the AEVs' routes. To the best of our knowledge, this study is the first attempt to formulate and solve the min-max version of AEVRP. We propose an efficient mixed-integer programming (MIP) formulation to solve small-scale instances. For large-scale instances, we develop a Genetic Algorithm-based Heuristic (GAH) with three phases. Extensive computational experiments evaluate all the proposed approaches.

The contributions of this study include the following: 1) an efficient MIP formulation for the AEVRP; 2) a GA-based heuristic for large-scale instances and extensive computational experiments to quantify the efficacy of the proposed approach; 3) computational experiments for MIP formulation using branch and cut algorithm; 4) a sensitivity analysis to investigate the aspects of solutions from min-sum and min-max AEVRP; and 5) a data-driven simulation study implemented with the robot operating system ROS middleware.

The remainder of this paper is organized as follows: Section II provides a mathematical formulation of the problem along with a subsequent reformulation. Section III introduces the solution methodologies where we present exact and heuristic

methods to solve small and large-scale instances, respectively. Section IV presents extensive computational experiments and sensitivity analysis. Finally, Section V provides concluding remarks.

II. MODEL FORMULATION

A. Problem Definition

We define T as a set of targets, and \bar{D} as a set of CSs. Define $D = \bar{D} \cup d_0$, be a set of CSs, including a depot d_0 where m AEVs are initially stationed, and each AEV is charged to its battery capacity. The AEVRP is defined on a directed graph with a set of vertices V and a set of edges E as $G = (V, E)$ where $V = T \cup D$. We assume that the graph G does not contain any self-loop. Each edge $(i, j) \in E$ is associated with a distance c_{ij} between vertices i and j , and f_{ij}^m is the charge consumed by traveling from i to j by an AEV m . The f_{ij}^m is calculated by multiplying the energy consumption rate of AEV m and c_{ij} . It is also assumed that both the distances and the charge costs satisfy the triangle inequality, e.g., $\forall i, j, k \in V$, $f_{ij}^m + f_{jk}^m \geq f_{ik}^m$. Also, let F_m denote the maximum charging capacity of any AEV m . The objective of the model is to find a route for each AEV starting and ending at the base depot such that: each target is visited at least once by an AEV; no AEV runs out of charge during the trip; and maximum distance traveled by an AEV is minimized.

B. Notation

- Sets
 - T : Set of targets, indexed as $t \in T$.
 - \bar{D} : Set of charging stations, indexed as $d \in \bar{D}$.
 - D : Set of charging stations and base depot, $D = \bar{D} \cup \{d_0\}$.
 - V : Set of all vertices in the graph, including all targets, CSs and base depot, $V = T \cup D$.
 - E : Set of all edges connecting any two vertices without any self-loop, $(i, j) \in E$ and $i, j \in V$.
 - S : Subset of targets and a depot in V , $S \subset V$, $\sigma^+(S) = \{(i, j) \in E : i \in S, j \notin S\}$.
 - M : Set of AEVs which are initially stationed at base depot d_0 , indexed by $m \in M$.
- Model parameters
 - c_{ij} : Distance associated with edge $(i, j) \in E$.
 - f_{ij}^m : Amount of charge spent by an AEV $m \in M$ while traversing from i to j with $i, j \in V$.
 - F_m : Battery capacity of AEV m , with $m \in M$.
 - q : A large constant, set as number of targets.
- Decision variables
 - x_{ij}^m : 1 if the edge (i, j) is traversed by an AEV m , and 0 otherwise;
 - z_{ij}^m : The total battery charge spent by any AEV m since the start from base depot or a CS and reaches the vertex $j \in V$ while the predecessor of j is $i \in V$.
 - y_d^m : 1 if the CS $d \in D$ is visited by any AEV m , and 0 otherwise.

C. Min-max AEVRP Model

$$\text{Min} \left(\text{Max}_{m \in M} \sum_{(i,j) \in E} c_{ij} x_{ij}^m \right) \quad (1)$$

s.t.

$$\sum_{i \in V} x_{di}^m = \sum_{i \in V} x_{id}^m \quad \forall d \in \bar{D}, m \in M, \quad (2)$$

$$\sum_{i \in V} x_{di}^m \leq q \cdot y_d^m \quad \forall d \in \bar{D}, m \in M, \quad (3)$$

$$\sum_{i \in V} x_{id_0}^m = 1, \sum_{i \in V} x_{d_0i}^m = 1 \quad \forall m \in M, \quad (4)$$

$$\sum_{i \in V} \sum_{m \in M} x_{ij}^m = 1, \sum_{i \in V} \sum_{m \in M} x_{ji}^m = 1 \quad \forall j \in T, \quad (5)$$

$$x(\sigma^+(S)) \geq y_d \quad \forall d \in S \cap \bar{D}, S \subset V \setminus \{d_0\} : S \cap \bar{D} \neq \emptyset, \quad (6)$$

$$\sum_{j \in V} z_{ij}^m - \sum_{j \in V} z_{ji}^m = \sum_{j \in V} f_{ij}^m x_{ij}^m \quad \forall i \in T, m \in M, \quad (7)$$

$$z_{ij}^m \leq F_m x_{ij}^m \quad \forall (i, j) \in E, m \in M, \quad (8)$$

$$z_{di}^m = f_{di}^m x_{di}^m \quad \forall i \in T, d \in D, m \in M, \quad (9)$$

$$x_{ij}^m \in \{0, 1\}, z_{ij}^m \geq 0 \quad \forall (i, j) \in E, m \in M, \quad (10)$$

$$y_d^m \in \{0, 1\} \quad \forall d \in \bar{D}, m \in M. \quad (11)$$

The objective function (1) minimizes the maximum distance traveled by any AEV. Constraints (2) impose the in-degree and out-degree of any AEV using a CS, d , to be equal. Constraints (3) are indicative where the variable y_d^m will be one if CS d is visited. Constraints (4) ensure that AEVs start and end their trip from the base depot d_0 . Constraints (5) force the in-degree and out-degree of each target to be equal, and each target should be visited by exactly one AEV. Connectivity of any feasible solution is guaranteed by constraints (6). Constraints (7) introduce the flow variable z_{ij}^m for each edge $(i, j) \in E$ and also removes the sub-tours. Constraints (8) and (9) ensure that no AEV runs out of charge during its trip. Finally, constraints (10) and (11) define the restrictions for the decision variables.

The model is non-linear due to the min-max term in the objective function (1). To improve computational efficiency, the model is linearized using the following proposition.

Proposition II.1. *Define a non-negative continuous variable w and restate the objective function as follows:*

$$\text{Min } w \quad (12)$$

Then, add the following constraint:

$$w \geq \sum_{(i,j) \in E} c_{ij} x_{ij}^m \quad \forall m \in M. \quad (13)$$

Proof. See [25] for the proof. \square

III. METHODOLOGY AND ALGORITHM DEVELOPMENT

A. Branch and Cut Algorithm

In this section, we describe the main components of a branch-and-cut algorithm used to optimally solve the formulation presented in Section II. To remove the binary restrictions for the variables y , following proposition is used.

Proposition III.1. *Relax the binary restrictions on constraints (11), and replace (3) and (11) by the following constraints:*

$$x_{di}^m \leq y_d^m \quad \forall i \in T \cup \{d_0\} \quad d \in \bar{D}, m \in M, \quad (14)$$

$$0 \leq y_d^m \leq 1 \quad \forall d \in \bar{D}, m \in M. \quad (15)$$

Proof. See [7] for the proof. \square

The majority of previous studies use a set of dummy binary variables for CSs, to maintain the connectivity of the AEV tours ([8], [17], [26]), that should be determined prior to the optimization by the users. This formulation can significantly increase the computational effort due to poor LP-relaxation. However, our formulation contains constraints (6) to guarantee the connectivity of any feasible solution without using dummy binary variables. But, the number of such constraints is exponential, and it may not be computationally efficient to consider all these constraints in advance while using an off-the-shelf solver. To address this issue, we relax the constraints (6) from the formulation. Whenever there is a feasible integer solution, we check if any of the constraints (6) are violated. If so, we add the corresponding constraint and continue solving the problem. It has been observed that this process is computationally efficient for a variety of the VRP problems [27], [28].

Now, we describe the details about the algorithm used to find a constraint (6) that is violated for a given integer feasible solution to the relaxed problem. For every AEV $m \in M$, a violated constraint (6) can be denoted by a subset of vertices $S \subset V \setminus \{d_0\}$ such that $S \cap \bar{D} \neq \emptyset$; and $x(\sigma^+(S)) < y_d^m$ for every $d \in S \cap \bar{D}$. We construct an auxiliary graph $G' = (V', E')$ for any feasible solution where $V' = T \cup d_0 \cup \{d \in \bar{D} : y_d^m = 1\}$, and $E' = \{(i, j) \in E : x_{ij}^m = 1\}$. We then find the Strongly Connected Components (SCC) of this graph. Every SCC sub-graph which does not contain the base depot d_0 violates the constraint (6). Hence, we add all these constraints for any feasible integer solution until we reach optimality. To implement this algorithm within the branch and cut framework, we use the *Callback* feature provided by most of the commercial solvers like Gurobi [29]. Although the branch-and-cut can find an optimal solution, the AEVRP is an extension of VRP problem and it is NP-hard [17]. Thus, to circumvent computational challenges for large-scale instances, we develop a heuristic method in the next section.

B. GA-based Heuristic Method

Genetic algorithms are a stochastic meta-heuristic technique inspired by the process of natural selection, which is widely applied to solve different classes of NP-Hard problems [30]. To solve the AEVRP using a GA algorithm, we have three major challenges: 1) assigning targets to the AEVs; 2) finding the best route for each AEV; and 3) maintaining feasibility such that each AEV does not run out of fuel. Each of these is complex, hence a naive GA may not be sufficient. Therefore, we implemented genetic algorithm based heuristic (GAH) in three different phases to produce good quality solutions.

The flowchart of GAH for the AEVRP is shown in Fig. 2. The algorithm initializes by computing a modified traveling cost matrix for each AEV to consider the charging limitation

of AEVs. Subsequently, a linear programming (LP) relaxation of an assignment problem is solved to assign the targets to the AEVs. Then, an optimal or a sub-optimal travelling salesman problem (TSP) tour for the AEVs is determined by the Lin-Kernigan-Helgaun heuristic [31]. In the next step, the feasibility of each route in terms of charge limitation is checked. On every infeasible route, a heuristic is applied to find CSs for recharging and the distance traveled by each AEV is calculated, and hence an initial solution is obtained. For a pool of high-quality solutions, an iterative Variable Neighborhood Search (VNS) is implemented, and uses the initial solution as the incumbent. Three different insertions are used to improve the incumbent solution. At each iteration, a new solution is generated and compared to the incumbent. If the new solution is better than the incumbent, it is considered as the ‘new’ incumbent and added to the GA pool. Also, if a new solution is not better but has a cost relatively close when compared to the incumbent, it is considered as a potentially good solution and added to the GA pool. This process is repeated until either no improvement is found or the maximum number of iterations is reached.

Once the GA pool is filled with high-quality solutions from VNS, the GA parameters such as the iteration number, population size, crossover rate, mutation rate, stopping criteria are initialized. The solutions in the pool represent GA chromosomes, and the fitness value of chromosomes is considered as the maximum distance traveled by any AEV. The chromosomes are sorted based on their fitness value and the ones with the higher fitness values are eliminated based on fixed population size. During the improvement phase, through a roulette wheel selection operation, some chromosomes are selected for the GA operations. The GA operations, such as crossover and mutation, are performed to generate new solutions (offsprings). The routing and feasibility check are performed again on the offsprings. The fitness value of the feasible offsprings is measured and compared to other chromosomes. These steps constitute an iteration, and then the roulette wheel selection is applied again to begin the next iteration. The GAH is terminated whenever a stopping criterion is met. In the post improvement, a heuristic is used on some of the best chromosomes to further improve the solution from the improvement phase. Steps of GAH are explained in the subsequent sections.

1) *Construction Phase*: The goal of construction phase is to produce high-quality feasible solutions as initial solutions for the AEVRP. For this purpose, we develop multiple heuristics and elaborate the details in the following sections.

a) *Path Representation*: To encode the solution of the AEVRP problem, we use path representation in a way that targets are listed based on the order in which they are visited. Suppose that there are 10 targets and numbered from t_5 to t_{14} . In order to form a chromosome, we generate a path where targets are randomly placed in each gene of the chromosome. A sample chromosome of AEVRP problem is as follows:

t_{10}	t_7	t_{11}	t_{12}	t_9	t_5	t_6	t_8	t_{13}	t_{14}
----------	-------	----------	----------	-------	-------	-------	-------	----------	----------

Note that each chromosome contains $|M|$ string, each related to an AEV.

b) *Modified Cost Matrix*: In this step, considering the range limitation of AEVs, we compute a new traveling cost based on [32]. The new cost matrix considers the additional charge that an AEV may need to visit the available CSs as it traverses between two targets. The maximum charge remaining at the AEV’s battery when it visits a target i is denoted as $F - f_{d_i}^{min}$ where $f_{d_i}^{min}$ denotes the amount of fuel an AEV requires to reach a CS with the minimum distance from target i . This ensures that in any feasible tour, an AEV must have an option of recharging at the nearest CS to continue visiting other targets when it reaches a target i . So, we say that an AEV can directly travel from target i to target j if and only if $f_{ij} \leq F - f_{d_i}^{min} - f_{d_j}^{min}$. If the AEV is unable to directly travel from target i to j , we create an auxiliary graph $G^* = (V^*, E^*)$ where $V^* = \bar{D} \cup \{i, j\}$. Any edge that can satisfy the fuel constraint will be added to the auxiliary graph. So, we add the following three sets of edges to the graph:

$$E^* =: \begin{cases} (i, d) : & \text{if } f_{id} \leq F - f_{d_i}^{min}, \forall d \in \bar{D}, \\ \cup (d, j) : & \text{if } f_{dj} \leq F - f_{d_j}^{min}, \forall d \in \bar{D}, \\ \cup (d_k, d_{k'}) : & \text{if } f_{d_k d_{k'}} \leq F, \forall d_k, d_{k'} \in \bar{D}. \end{cases}$$

For every AEV, the cost (length) of the edges in the graph E^* is calculated by finding the shortest path between the any two nodes using Dijkstra’s Algorithm [33]. The modified cost matrix is created by replacing the new computed costs with old costs in the original cost matrix. We denote the modified cost vector as c' .

c) *Target Assignment and Routing*: To initially assign targets to the AEVs, we use a LP-based Load Balancing heuristic (LLBH) as suggested in [34] with some modifications. The LLBH assumes that the distance traveled by the AEVs should almost be the same, and designed for multi-depot problems. Hence, in a network where targets are uniformly distributed, AEVs visit nearly the same number of targets. For the sake of compatibility, we perturb the location of AEV in the base depot to create multiple depots. We uniformly place the AEVs on a small circle around the base depot (Fig. 3). Given a set of K base depots, indexed by i , with one AEV stationed at each of them, and set of t targets, indexed by j , the LLBH solves the relaxation of the following assignment problem where u_{ij} is 1 if target j is assigned to the depot i , and 0 otherwise. Also, c'_{ij} indicates the modified cost matrix.

$$\mathbf{P}: \text{Min} \sum_{i \in K} \sum_{j \in T} c'_{ij} u_{ij} \quad (16)$$

s.t.

$$\sum_{i \in K} u_{ij} = 1 \quad \forall j \in T, \quad (17)$$

$$\sum_{j \in T} u_{ij} = \lfloor \frac{|T|}{K} \rfloor \quad \forall i \in K, \quad (18)$$

$$u_{ij} \in \{0, 1\} \quad \forall i \in K, j \in T. \quad (19)$$

Constraints (17) assign targets to the ‘ K ’ copies of depots made around the base depot d_0 . Constraints (18) determine the number of targets that each AEV should visit. For the cases where $\frac{|T|}{K}$ is fractional, as per [34] we assume that

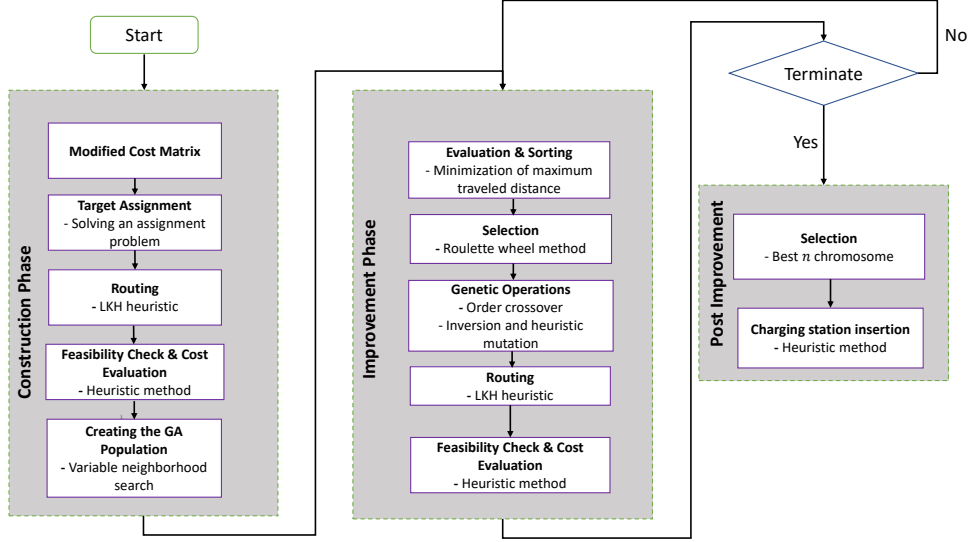


Fig. 2: Flowchart of the GAH approach including the three main phases: construction, improvement and post improvement.

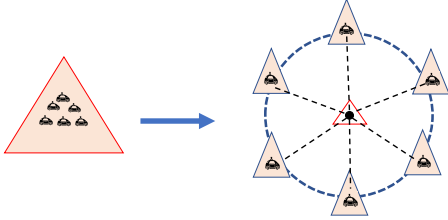


Fig. 3: Conversion of single depot to multi-depots using perturbation method.

$|T| = pK + r$, with $p, r \in \mathbb{Z}^+$ and r is residue. The extra r targets are assigned to the AEVs based on a saving technique which we describe in the next sections. After the initial assignment of targets to AEVs by solving \mathbf{P} , the auxiliary depots are removed. Then, we add the base depot (d_0) to the beginning and end of each route which result in a group of strings. Now, we solve a single AEV routing problem for every set of targets assigned to each AEV including the base depot using the Lin-Kernigan-Helgaun (LKH). LKH is considered as one of the best algorithms for solving single vehicle routing problem without recharging constraints.

d) Feasibility Check: The route found by LKH heuristic for each AEV may be infeasible due to the exclusion of range constraint (8). Hence, this step is performed to attain feasibility for the tours. We calculate the charge consumption of the AEVs as they traverse along their route. Whenever the charge consumption exceeds the battery capacity, we stop at the last target (e.g. t_i) that AEV visited before recharging. At this step, a CS should be selected for recharging. The algorithm developed by [26] considers the minimum of $dist(t_i, d_k) \forall k \in \bar{D}$, where ‘ $dist$ ’ represent distances based on the parameter f . However, in this work, we choose the minimum of $dist(t_{i+1}, d_k) \forall k \in \bar{D}$. The advantage of this approach is that the AEV will have more charge to complete the rest of the trip, and also has less necessity for recharging. Consequently, this may lead to shorter distance traveled. However, if the AEV

does not have sufficient charge to reach d_k , then the minimum of $dist(t_i, d_{k'}) \forall k' \in \bar{D} \setminus \{k\}$ is selected for recharging. If visiting $d_{k'}$ is also not possible, then we do a “backward” move and go to the previous edge (t_{i-1}, t_i) and perform the same approach. We call a route infeasible if one of the following circumstances occurs: 1) backward moves resulted in visiting the base depot; 2) all the available CSs in one edge are visited and yet it is impossible to move to the next edge; or 3) exiting from a target is impossible due to insufficient charge, and also the closet CS to the target is visited in the previous edge.

The feasibility procedure is applied on every route to create a feasible solution along with its corresponding cost for the min-max AEVRP problem. This solution x is considered as the incumbent solution, $x_{inc} = x$.

e) Variable Neighborhood Search (VNS): To create a pool of high-quality solutions for the GA, we implement a VNS-based algorithm. The VNS framework is based on a systematic change of neighborhood integrated with a local search [35]. A local search starts with an initial solution x_{inc} and looks for a descent direction from x within a neighborhood $N(x)$. The algorithm stops if there is no further improvement. In this problem, we consider four neighborhoods including one, two, and three insertions which we refer as $N_1(x)$, $N_2(x)$ and $N_3(x)$, respectively, and swap operation as $N_4(x)$. In the insertion procedure, we try to improve the initial solution by removing the target from the longest route (in terms of distance) and insert it to another route. Considering the initial solution obtained in the previous section, we generate a new solution x' from $N_1(x)$. In order to select the target for removal, we calculate the amount saved when removing each target from the longest route. The savings from removing target i is calculated as follows:

$$dist(t_j, t_i) + dist(t_i, t_k) - dist(t_j, t_k), \quad (20)$$

where t_j and t_k are the preceding and succeeding targets in the same route. We select the target with the highest savings

from the longest route to be inserted into another route.

In the next step, we determine the route on which we want to insert the target. We compute the insertion cost of the selected target in other routes and select the route with the minimum insertion cost. The insertion cost of each route is calculated based on the equation (20) where t_i is inserted between any two consecutive targets t_j and t_k from the route. Then, we apply the LKH and feasibility check on the new solution. If $f(x') < f(x_{inc})$ then $x_{inc} = x'$, where $f(\cdot)$ is the objective function represented in (1). The procedure continues with a new solution from $N_1(x')$, otherwise, we select the next target with the highest savings. If there is no improvement by removing any target from the longest route and inserting into another route, we create a new solution from $N_2(x)$ and proceed.

Whenever we find a better solution from $N_2(x)$, we return to the 1-insertion neighborhood and restart the process. Otherwise, we proceed by selecting another target. If there is no improvement in the 2-insertion neighborhood, we activate the $N_3(x)$ and proceed as before. We also use the swap operation $N_4(x)$ by randomly selecting a target from the longest route and exchanging it with any target from the route with the lowest insertion cost to further improve the solution. The swap operation is activated between any insertion operations (among $N_1(x)$, $N_2(x)$, and $N_3(x)$) and repeated for a predetermined number of iterations (l_{max}). We terminate the search if no improvement occurs in the 3-insertion neighborhood or the maximum number of iterations is reached. It should be noted that the saving and insertion cost calculations are based on the modified cost matrix. The VNS algorithm procedure is summarized in the Algorithm 1.

Algorithm 1 : Variable Neighborhood Search

Initialization:

$k, l \leftarrow 0, x_{inc} \leftarrow x^0, N_1 \leftarrow \text{True}, N_2 \leftarrow \text{False},$
 $N_3 \leftarrow \text{False}, i \leftarrow 1$

while $k \leq k_{max}$:

while $N_i = \text{True}$

$k \leftarrow k + 1$

 select $x' \in N_i(x_{inc})$

if $f(x') \leq f(x_{inc})$:

$x_{inc} = x', i \leftarrow 1$

if $\nexists x \in \{x' | x' \in N_i(x'), f(x') \leq f(x_{inc})\}$:

$N_i \leftarrow \text{False}$

$i \leftarrow i + 1, N_i \leftarrow \text{True}$

while $l < l_{max}$

 do swap , $l \leftarrow l + 1$

During the search process, every new solution is added to the GA pool. Inspired from simulated annealing, potentially good solutions are stored. A solution is potentially good if $\frac{f(x') - f(x_{inc})}{f(x_{inc})} \leq s$, where $f(x')$ and $f(x_{inc})$ are the costs of the potentially good and incumbent solutions, and s is a relatively small parameter (e.g., $s=0.15$ in our implementation). In the next step, we apply the GA operations on the pool of high quality solutions.

C. Improvement Phase

1) *Chromosome Selection*: Chromosome selection significantly affects the GAH's convergence. The roulette wheel selection was first introduced by [36] to select the chromosomes for GA operations. Each section of the roulette wheel is assigned to a chromosome based on the magnitude of its fitness value. The fitness value of each chromosome is based on objective function value given in (1) for each AEV m . The fitness values of the chromosomes determine their chance of being selected.

2) *Crossover and Mutation*: We apply two approaches to diversifying the solution space. The first approach is order crossover introduced in [37] to sample and combine selections from different potential solutions. In this approach, two offsprings are generated in each iteration by choosing a sub-tour of one parent and maintaining the relative sequence of genes of another parent. The second approach is a form of mutation, which is a genetic operator that reorders some of the gene values in a chromosome from their existing state. We apply heuristic and inversion mutation proposed by [37]. In the heuristic mutation, three genes are randomly selected from each parent, and all the possible combinations of the selected genes are generated. The best chromosome is considered as the offspring. In the inversion mutation, a sub-string of a parent chromosome is selected and used to produce an offspring.

3) *Post Improvement*: The GA algorithm returns the best set of chromosomes after any of the predefined stopping criteria is met. In the feasibility heuristic, an insertion of a CS is performed whenever a recharging is required. A route for an AEV is defined as a sequence of targets and CSs ($d_0, t_i, t_j, d_n, \dots, t_l, d_m, \dots, d_0$) where d_0 , denotes the base depot and $i, j, l \in V$ and $m, n \in \bar{D}$. In some instances, it is possible to obtain a better fitness value by changing the position of the CSs in chromosomes. To further enhance the quality of the GA solution, we propose a heuristic which is described by an example as follows: suppose that there are three CSs (d_1, d_2 , and d_3), and the following string is a feasible path for an AEV (the visited CSs are colored with red):

d_0	t_8	t_{11}	d_3	t_9	t_5	d_2	d_0
-------	-------	----------	-------	-------	-------	-------	-------

Here we define the ‘‘sub-string’’ as a sequence of visits where the last node is a CS. We select the first sub-string and delete the CS from the sub-string. We then insert all the eligible CSs among the targets to generate new sub-routes. A CS is considered eligible if the AEV starting from a target can reach that CS without visiting other CSs and also could reach the next target after recharging. New sub-routes are checked for battery capacity violation. The total distance traveled and the AEV's remaining battery charge are stored for each feasible route. This considerably decreases the computational effort. The left table in Fig. 4 shows all the new sub-routes generated by CS insertion, where the feasible sub-routes are highlighted. Then, we delete the infeasible sub-routes and add the second sub-string. We repeat the same CS insertion procedure for the second sub-string using the information stored in the previous step. The final possible routes are shown in the right table in Fig. 4.

d_0	d_1	t_8	t_{11}	t_9					
d_0	t_8	d_1	t_{11}	t_9					
d_0	t_8	t_{11}	d_1	t_9					
d_0	d_2	t_8	t_{11}	t_9					
d_0	t_8	d_2	t_{11}	t_9					
d_0	d_3	t_8	t_{11}	t_9					
d_0	t_8	t_{11}	d_3	t_9					

d_0	d_1	t_8	t_{11}	t_9	d_1	t_5	d_0
d_0	t_8	t_{11}	d_1	t_9	t_5	d_1	d_0
d_0	d_3	t_8	t_{11}	t_9	d_2	t_5	d_0
d_0	t_8	t_{11}	d_3	t_9	t_5	d_2	d_0
d_0	t_8	t_{11}	d_3	t_9	d_3	t_5	d_0
d_0	t_8	t_{11}	d_3	t_9	t_5	d_3	d_0

Fig. 4: Initial sub-tours generated in the first step of CS insertion heuristic (left table), and final feasible routes (right table).

We continue the procedure to visit the last node in all routes. Then the feasible route with the lowest distance is considered as the AEV's total traveled distance. It should be noted that since the heuristic does not change the order of the targets, the chromosome remains the same. So, we use this heuristic only on final n best chromosomes returned by GA algorithm, where n is a predefined user parameter (e.g., in this work we used $n=15$).

IV. EXPERIMENTS AND RESULTS

In this section, we compare the computational performance of the B&C algorithm and the GAH approach. All the experiments were implemented in Python 3.7, and the MIP models were solved by Gurobi 9.0 using a computer with an Intel (®) Xeon (®) CPU E5-2640, 2.60 GHz, and 80GB RAM.

A. Instance Generation

For the computational experiments, we selected three data sets (A, B, and P) of the capacitated vehicle routing problem developed by Augerat et al. [38]. We then modified the data sets to adapt for AEVRP by adding CSs. We also generated a random data set to maintain the diversity in our experiments. The details of the data sets are as follows:

- *Random instances:* Random instances were generated in a square grid of size [100, 100], and the base depot at (50, 50). The number of CSs was set to five, and the locations of the depot as well as the charging stations were fixed as apriori for all the random test instances. The number of targets varies from 10 to 50 in steps of five, while their locations were uniformly distributed within the square grid. For each of the generated instances, the number of AEVs in the base depot is varied from two to eight. The battery capacity of AEVs was set to 100, and the Energy Consumption Rate is considered to be 0.8.
- *Augerat et al. instances:* The data sets reported in the study by Augerat et al. [38] are developed for capacitated vehicle routing problems. These instances include three sets which differ in distribution and number of targets, vehicle's capacity, demand/capacity, and number of vehicles. To make the instances compatible to AEVRP, we added five CSs. The coordination of CSs are similar for all instances within each data set. Also, the capacity of vehicles is considered as the battery capacity of AEVs and capacity tightness as the fuel consumption rate in our problem. Fig. 5 shows the four different data sets.

B. Experiment on AEVRP Instances

1) *Benchmark Instances:* To create benchmark instances, we selected a subset of targets, the first 10 and 15 targets

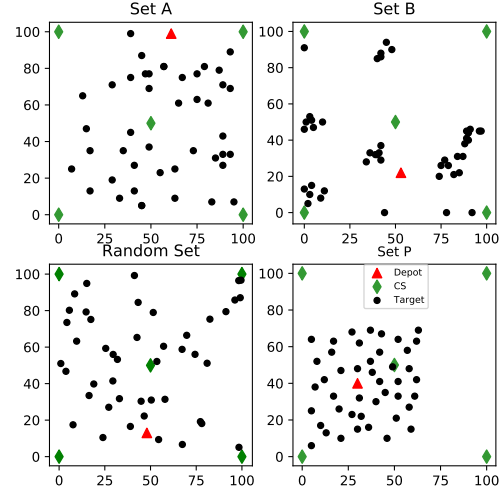


Fig. 5: Four different data sets generated based on the study in [38].

with two and three AEVs from instances within each data set, respectively. We solved the benchmark instances with GAH and compared the obtained results to the optimal or near-optimal solution solved by the B&C procedure. Fig. 6 represents the differences in the objective function between GAH and B&C for the 10-target and 15-target instances. The difference in objective percentage and run-time in seconds are calculated as $\frac{B\&C(O) - GAH(O)}{B\&C(O)} \times 100$, and $(B\&C(t) - GAH(t))$, where $B\&C(O)$ and $GAH(O)$ indicate objective values, and $B\&C(t)$ and $GAH(t)$ indicate the run-time of B&C and GAH, respectively. In total, 71 10-targets and 71 15-targets benchmark instances were solved. For all the 10-target instances, the B&C algorithm was able to reach solutions within 1% of the optimality gap. For many of the 15-target instances from sets A, B, and Random, the B&C algorithm was not able to find the optimal solution within the stipulated time limit of two hours. However, B&C found the optimal solution for most of the 15-target instances from set P. Fig. 6 represents the runtime and objective function differences between GAH and B&C. For all the completed runs using B&C, the GAH reached the optimal solution or near-optimal solution with less than 2.5% gap. For the instances where B&C was not able to reach optimality, the GAH approach could find a solution closer or better compared to the upper bound provided by B&C. In terms of run-time, for more than half of the 10-target instances, GAH outperformed B&C. Also, GAH outperformed B&C with a much better run-time in the experiments with 15-target instances. It should be noted that we removed the instances which reached the time-limit in Fig 6 using B&C to better illustrate the run-time difference in 15-target instances. The results from the benchmark instances indicate that the GAH approach is capable of providing highly efficient routes for AEVs.

2) *Large-scale Instances:* To demonstrate the performance of GAH on large scale problem sets, we considered 82 instances with the number of targets and AEVS up to 60 and 15, respectively. Among these instances, 18 instances are from set A, and 17, 12, and 35 instances are from sets B,

Table I: Characteristics of the large-scale instances for different data sets

Sets	Target range	Vehicles range	Consumption rate range	Battery Capacity range
A	[31,60]	[5,9]	[0.81,0.99]	100
B	[30,60]	[4,9]	[0.82,1]	100
P	[21,59]	[5,15]	[0.88,0.99]	[70,170]
Random	[20,50]	[4,10]	[0.8,0.8]	100

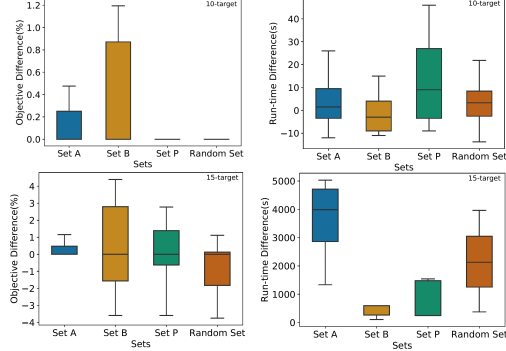


Fig. 6: Performance of the GAH compared to the B&C procedure for benchmark instances with 10 and 15 targets.

P, and Random, respectively. In 32 of the 82 total instances, B&C procedure was not able to find any feasible solution whereas GAH was capable of providing a feasible solution for all instances in just a few seconds. Table II represents the comparison between the B&C procedure and GAH for each set. The first column indicates the total number of instances, and the columns ‘# of Inf(B&C)’ and ‘# of Inf(GAH)’ indicate the number of instances in which the B&C procedure and GAH could not find any feasible solution in the stipulated time limit. The next two columns labeled ‘AG-B&C(%)’ and ‘ART-GAH(%)’ specify the average gap percentage and the average run-time in seconds obtained by the B&C and GAH approaches. The last column labeled ‘AOD(%)’ is the average objective difference percentage between B&C procedure and GAH. So, in reading across the first row of Table II, for the 18 instances in set A, the B&C procedure found a feasible solution for nine instances with an average optimality gap of 63.7%. While GAH found a feasible solution for all 18 instances. Similarly, for sets B, P, and Random, B&C procedure found a feasible solution for 5, 10 and 20 instances with an average gap of 51.3%, 35.3%, and 61.1%, respectively. For all the experiments using large-scale instances, GAH outperformed B&C procedure in terms of computational time and the quality of the solution. Fig. 7 illustrates the performance of GAH compared to the B&C algorithm, where the horizontal and vertical axes indicate the number of targets and the min-max objective for different instances. Also, the disconnected lines indicate the instances where the B&C could not find any feasible solutions within the time limit.

C. Sensitivity Analysis

1) *Effect of the Number of AEVs:* We analyze the effect of increasing in the number of AEVs on the objective function and the total distance traveled by all the AEVs. As shown in Fig. 8, when there is an increase in the number of AEVs, in general, the maximum distance traveled by the AEVs decreases. However, the total distance traveled by all the AEVs

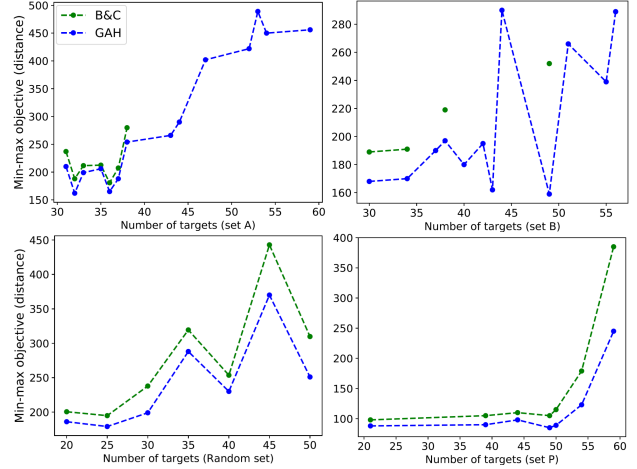


Fig. 7: Comparison between the performance of GAH and B&C for different large-scale instances.

increases. The instance from set B has the highest increase in the total distance traveled by the AEVs as the number of CSs increased. This result is likely due to the cluster-like distribution of the targets that occurred in that data set. When the number of AEVs surpasses the number of clusters, each cluster is assigned to more than one AEV which can increase the total distance. Another factor that may significantly affect the total distance is the position of the depot. In the cases where the depot is far from the targets, dispatching multiple AEVs could result in a longer total distance. Since the targets are closer to each other in set P, an increase in the number of AEVs would not result in a notable decrease or increase in the min-max or total distance, respectively. In conclusion, decision makers should evaluate the trade-off between the maximum and total distance considering the distribution of the targets and location of the depot.

2) *Effect of the Number of Charging Stations:* Another perspective is the impact of increase in the number of CSs on the min-max objective function. We chose an instance from each of the four data sets, and for each instance, we considered two to seven randomly placed CSs. Fig. 9 shows the effect of number of CSs on min-max AEVRP for different instances. An increase in the number of charging instances has a lower impact on sets P and B sets where the targets are condensed in a smaller area. Due to the scattered distribution of the targets in the random set and set A, we observe a rapid decrease in the maximum distance as the number of charging stations decreases. Logistics companies should evaluate the marginal benefits of adding more CSs based on the distribution of the customers in their network.

Table II: Comparison of the performances of GAH and B&C procedure for large-scale instances

Sets	# of Instances	# of Inf(B&C)	# of Inf(GAH)	AG-B&C(%)	ART-GAH(s)	AOD(%)
A	18	9	0	63.7	290	17.1
B	17	12	0	51.3	246	16.8
P	12	2	0	35.3	228	18.2
Random	35	5	0	61.1	283	21

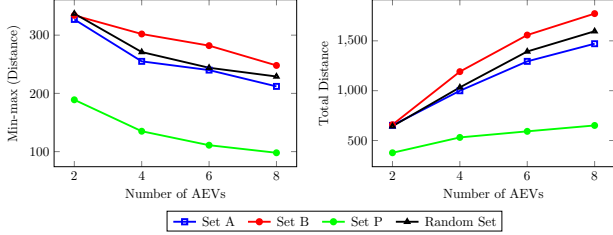


Fig. 8: Effect of increase in the number of AEVs on the min-max and the total distance traveled by the AEVs.

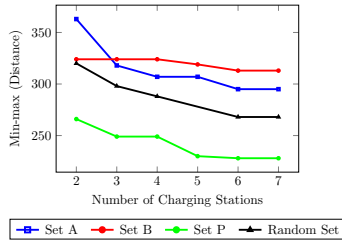


Fig. 9: Effect of increase in the number of charging stations on sets A, B, P and Random.

D. Data-driven Simulation

Finally, we performed a data-driven simulation study using the Rviz [39] 3D-simulation environment for the robotic operating system (ROS) [40] middleware to showcase the application of AEVRP for robots. We used Turtlebots [41] from the turtlebot_stage package environment as shown in Fig. 10. The black oval indicates the base depot where the Turtlebots are stationed. The red rectangles indicate targets, and the blue circles represent the charging locations. The highlighted black lines are walls (obstacles) that prevent Turtlebots from moving from one target to another directly. The ROS navigation stack computes the distance between any pair of targets and depots in the environment. However, it is not possible to use the distance matrix in the AEVRP model since it does not satisfy the triangle inequality. Hence, to preserve the triangle inequality, we converted the distance between each pair of nodes calculated by ROS denoted as f'_{ij} to f_{ij} using Dijkstra's algorithm [33]. The Dijkstra algorithm creates a mapping between f'_{ij} to f_{ij} by calculating the shortest path between nodes. We use the new distance matrix as the cost to the AEVRP problem and conducted experiments with four different instances. In each instance, there are two Turtlebots, nine targets, and five charging locations. The experiments were performed using ROS Kinetic Kame [42] using a Ubuntu 16.04 (Xenial) release and the ROS publishers were developed using the Python programming language. Fig. 11 shows the traveled distance by each turtlebot for min-max and min-sum

AEVRP with two and three turtlebots. In the instances 1 and 2 with two turtlebots, we observe the total distance traveled by Turtlebots are same, however, a significant difference between the traveled distance for each Turtlebot in the min-max versus min-sum. In instances 3 and 4, we notice a slight increase in the total traveled distance in min-max but considerable improvement in the workload balancing between the two Turtlebots. A similar pattern is observed in the experiment with three Turtlebots. In summary, on average, we observed a 2% increase in the total traveled distance by the Turtlebots using the min-max, however a 95% improvement in balancing the traveled distance between the Turtlebots while compared to the min-sum AEVRP.

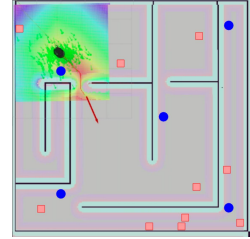


Fig. 10: Rviz navigation environment illustrated using Turtlebot package.

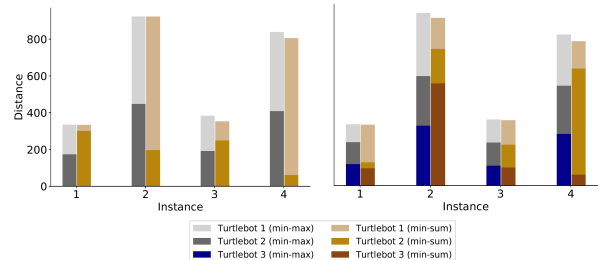


Fig. 11: Comparison among four different instances for total distance and workload balance for two (left), and three (right) turtlebots using min-max and min-sum approaches.

V. CONCLUSION

In this research, we consider a min-max routing problem for a fleet of AEVs in the presence of charging stations. We proposed an efficient mixed-integer programming formulation and a genetic algorithm based heuristic to solve small and large-scale instances, respectively. Numerical studies are performed on randomly generated data sets and capacitated vehicle routing problem data sets from literature. The efficacy of the proposed methods are benchmarked using extensive computational experiments. The results indicate that GAH was able to find solutions within 1% of the optimality gap for the 10-target, and equal or better solutions in the 15-target benchmark instances. Also, GA-based heuristic could produce high-quality solutions in large-scale instances whereas the branch-and-cut procedure could not even find a feasible

solution for most of the instances within the two hours time limit. The proposed methods are capable for facilitating routing and charging decisions for a fleet of AEVs employed by logistics and transportation companies. The sensitivity analysis indicates that with a reasonable sacrifice in the total distance, the proposed approach can significantly decrease the travel time to visit some of the targets. In addition, this may decrease the maintenance cost of the AEVs due to fair and equitable distribution of workload among the AEVs fleet. This could potentially decrease the aging or degradation of batteries in AEVs. In addition, we conducted a data-driven simulation using the ROS package to investigate the application of the AEVRP for robots. Future work could include AEVs with freight capacities and the targets with time windows. Another extension could be incorporating uncertainties in the battery consumption rate as well as the location of target locations especially for surveillance applications. From an algorithmic perspective, use of decomposition algorithms like the column generation method can also be investigated.

REFERENCES

- [1] H. Nazaripouya, B. Wang, and D. Black, "Electric vehicles and climate change: Additional contribution and improved economic justification," *IEEE Electrification Magazine*, vol. 7, no. 2, pp. 33–39, 2019.
- [2] S. Solaymani, "Co2 emissions patterns in 7 top carbon emitter economies: The case of transport sector," *Energy*, vol. 168, pp. 989–1001, 2019.
- [3] J. Wu, H. Liao, J.-W. Wang, and T. Chen, "The role of environmental concern in the public acceptance of autonomous electric vehicles: A survey from china," *Transp Res Part F Traffic Psychol Behav*, vol. 60, pp. 37–46, 2019.
- [4] Z. Yi, J. Smart, and M. Shirk, "Energy impact evaluation for eco-routing and charging of autonomous electric vehicle fleet: Ambient temperature consideration," *Transp. Res. Part C Emerg. Technol.*, vol. 89, pp. 344–363, 2018.
- [5] T. D. Chen and K. M. Kockelman, "Management of a shared autonomous electric vehicle fleet: Implications of pricing schemes," *Transportation Research Record*, vol. 2572, no. 1, pp. 37–46, 2016.
- [6] H. Zhang, C. J. Sheppard, T. E. Lipman, and S. J. Moura, "Joint fleet sizing and charging system planning for autonomous electric vehicles," *IEEE trans Intell Transp Syst*, 2019.
- [7] K. Sundar, S. Venkatachalam, and S. Rathinam, "An exact algorithm for a fuel-constrained autonomous vehicle path planning problem," *arXiv preprint arXiv:1604.08464*, 2016.
- [8] M. Schneider, A. Stenger, and D. Goeke, "The electric vehicle-routing problem with time windows and recharging stations," *Transportation Science*, vol. 48, no. 4, pp. 500–520, 2014.
- [9] G. Hiermann, J. Puchinger, S. Ropke, and R. F. Hartl, "The electric fleet size and mix vehicle routing problem with time windows and recharging stations," *Eur. J. Oper. Res.*, vol. 252, no. 3, pp. 995–1018, 2016.
- [10] P. Slowik and N. Lutsey, "The continued transition to electric vehicles in us cities," 2018.
- [11] S. S. Fazeli, S. Venkatachalam, R. B. Chinnam, and A. Murat, "Two-stage stochastic choice modeling approach for electric vehicle charging station network design in urban communities," *IEEE trans Intell Transp Syst*, 2020.
- [12] Ç. Koç and I. Karaoglan, "The green vehicle routing problem: A heuristic based exact solution approach," *Appl. Soft Comput.*, vol. 39, pp. 154–164, 2016.
- [13] K. Sundar and S. Rathinam, "Algorithms for routing an unmanned aerial vehicle in the presence of refueling depots," *IEEE T AUTOM SCI ENG*, vol. 11, no. 1, pp. 287–294, 2013.
- [14] G. Desaulniers, F. Errico, S. Irnich, and M. Schneider, "Exact algorithms for electric vehicle-routing problems with time windows," *Operations Research*, vol. 64, no. 6, pp. 1388–1405, 2016.
- [15] F. Y. Vincent, A. P. Redi, Y. A. Hidayat, and O. J. Wibowo, "A simulated annealing heuristic for the hybrid vehicle routing problem," *Appl. Soft Comput.*, vol. 53, pp. 119–132, 2017.
- [16] A. A. Juan, J. Goentzel, and T. Bektaş, "Routing fleets with multiple driving ranges: Is it possible to use greener fleet configurations?," *Appl. Soft Comput.*, vol. 21, pp. 84–94, 2014.
- [17] S. Erdoğan and E. Miller-Hooks, "A green vehicle routing problem," *Transportation research part E: logistics and transportation review*, vol. 48, no. 1, pp. 100–114, 2012.
- [18] D. Levy, K. Sundar, and S. Rathinam, "Heuristics for routing heterogeneous unmanned vehicles with fuel constraints," *Mathematical Problems in Engineering*, vol. 2014, 2014.
- [19] B. Lunz, Z. Yan, J. B. Gerschler, and D. U. Sauer, "Influence of plug-in hybrid electric vehicle charging strategies on charging and battery degradation costs," *Energy Policy*, vol. 46, pp. 511–519, 2012.
- [20] A. M. Campbell, D. Vandenbussche, and W. Hermann, "Routing for relief efforts," *Transportation Science*, vol. 42, no. 2, pp. 127–145, 2008.
- [21] M. Torabbeigi, G. J. Lim, and S. J. Kim, "Drone delivery scheduling optimization considering payload-induced battery consumption rates," *J INTELL ROBOT SYST*, vol. 97, no. 3, pp. 471–487, 2020.
- [22] S. J. Zaloga, *Unmanned aerial vehicles: robotic air warfare 1917–2007*. Bloomsbury Publishing, 2011.
- [23] S. G. Manyam, D. W. Casbeer, and K. Sundar, "Path planning for cooperative routing of air-ground vehicles," in *2016 American Control Conference (ACC)*, pp. 4630–4635, IEEE, 2016.
- [24] A. C. Kapoutsis, S. A. Chatzichristofis, and E. B. Kosmatopoulos, "Darp: divide areas algorithm for optimal multi-robot coverage path planning," *J INTELL ROBOT SYST*, vol. 86, no. 3–4, pp. 663–680, 2017.
- [25] M. E. Posner and C.-T. Wu, "Linear max-min programming," *Mathematical Programming*, vol. 20, no. 1, pp. 166–172, 1981.
- [26] S. Zhang, Y. Gajpal, and S. Appadoo, "A meta-heuristic for capacitated green vehicle routing problem," *Annals of Operations Research*, vol. 269, no. 1–2, pp. 753–771, 2018.
- [27] K. Sundar, S. Venkatachalam, and S. G. Manyam, "Path planning for multiple heterogeneous unmanned vehicles with uncertain service times," in *2017 International Conference on Unmanned Aircraft Systems (ICUAS)*, pp. 480–487, IEEE, 2017.
- [28] S. Venkatachalam, M. Bansal, J. M. Smereka, and J. Lee, "Two-stage stochastic programming approach for path planning problems under travel time and availability uncertainties," *arXiv preprint arXiv:1910.04251*, 2019.
- [29] L. Gurobi Optimization, "Gurobi optimizer reference manual," 2020.
- [30] W. Ho, G. T. Ho, P. Ji, and H. C. Lau, "A hybrid genetic algorithm for the multi-depot vehicle routing problem," *Eng. Appl. Artif. Intell.*, vol. 21, no. 4, pp. 548–557, 2008.
- [31] K. Helsgaun, "An effective implementation of the lin–kernighan traveling salesman heuristic," *Eur. J. Oper. Res.*, vol. 126, no. 1, pp. 106–130, 2000.
- [32] S. Khuller, A. Malekian, and J. Mestre, "To fill or not to fill: the gas station problem," in *European Symposium on Algorithms*, pp. 534–545, Springer, 2007.
- [33] E. W. Dijkstra *et al.*, "A note on two problems in connexion with graphs," *Numerische mathematik*, vol. 1, no. 1, pp. 269–271, 1959.
- [34] J. Carlsson, D. Ge, A. Subramaniam, A. Wu, and Y. Ye, "Solving min-max multi-depot vehicle routing problem," *Lectures on global optimization*, vol. 55, pp. 31–46, 2009.
- [35] P. Hansen, N. Mladenović, and J. A. M. Pérez, "Variable neighbourhood search: methods and applications," *Ann. Oper. Res.*, vol. 175, no. 1, pp. 367–407, 2010.
- [36] L. Davis, "Applying adaptive algorithms to epistatic domains.," in *IJCAI*, vol. 85, pp. 162–164, 1985.
- [37] M. Gen and R. Cheng, *Genetic Algorithms and Manufacturing Systems Design*. John Wiley & Sons, Inc., 1996.
- [38] P. Augerat, J. M. Belenguer, E. Benavent, A. Corberán, D. Naddef, and G. Rinaldi, *Computational results with a branch and cut code for the capacitated vehicle routing problem*, vol. 34. IMAG, 1995.
- [39] D. Hershberger, D. Gossow, and J. Faust, "Rviz, 3d visualization tool for ros," URL: <http://wiki.ros.org/rviz> [cited 06-12-2020].
- [40] ROS, "Robot operating system," URL: <https://www.ros.org/> [cited 06-12-2020].
- [41] P. R. kit, "Turtlebot," URL: <https://www.turtlebot.com/> [cited 06-12-2020].
- [42] ROS, "Ros kinetic kame," URL: <http://wiki.ros.org/kinetic> [cited 06-12-2020].